

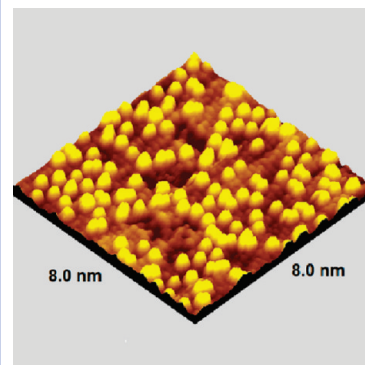
Formation of Pd Monomers and Dimers on a Single-Crystal Pd₃Fe(111) Surface

Xiaofang Yang,[†] Jun Hu,[‡] Ruqian Wu,[‡] and Bruce E. Koel*[†]

[†]Department of Chemistry, Center for Advanced Materials and Nanotechnology, Lehigh University, Bethlehem, Pennsylvania 18015, and [‡]Department of Physics and Astronomy, University of California, Irvine, California 92697

ABSTRACT Surface reconstruction of binary alloys is important in heterogeneous catalysis because it modifies both surface composition and structure and thus affects the catalytic activity and selectivity. We report here on segregation and surface morphology at a Pd₃Fe(111) single-crystal model catalyst investigated by low-energy ion scattering (LEIS) and scanning tunneling microscopy (STM). Annealing in vacuum causes Pd segregation, and STM reveals a complex surface structure with 0.17 monolayers of Pd monomer and dimer adatoms on top of the outermost alloy layer. This result is explained by density functional theory (DFT) calculations, which reveal that the contribution from vibrational free energy causes Pd atoms to detach from step edges at high temperature (> 1200 K) and then become trapped at room temperature at Fe defect sites due to a large diffusion barrier. This adlayer structure differs from surface structures observed for other binary alloy systems and is likely to offer new opportunities for manipulating catalytic properties of bimetallic alloys.

SECTION Surfaces, Interfaces, Catalysis



Pd–Fe bimetallic catalysts have been widely studied in heterogeneous catalysis for reactions such as selective hydrogenation of unsaturated hydrocarbons,^{1,2} production of methanol from synthesis gas,³ and improved oxygen reduction at the cathode in PEM fuel cells.^{4–6} It is well-known that the enhanced catalytic properties of bimetallic catalysts originate from both ligand effects and geometric effects.^{7,8} Ligand effects arise from modification of the electronic structure of the first metal by the second metal, in particular, the filling and shifting of their d states. Geometric effects are induced by changes in the arrangement of active sites (ensembles) that alters the transition states and hence the reaction kinematics. Basic information on composition and structure of bimetallic surfaces and how segregation in alloys influences their surface properties is of great importance for the control of catalytic properties.⁹

Herein, we show that the Pd₃Fe(111) surface may exhibit an unusual surface morphology, with Pd adatoms atop a Pd-enriched alloy surface, after a particular annealing procedure. This surface structure is different from other well-studied (111) surfaces of 3d and 4d alloys, such as Pd/M (M = Ni, Co) and Pt/M (M = Fe, Ni, Cu, Rh),¹⁰ which are comprised of flat and complete terraces after high-temperature annealing. The discovery of such a special structure for the Pd₃Fe(111) surface raises an interesting question of how to control the distribution of Pd adatoms for the optimization of catalytic properties of this alloy.

The clean Pd₃Fe(111) surface prepared by Ar⁺ ion sputtering and annealing to 1100 K exhibits a sharp and bright (1 × 1) hexagonal LEED pattern (Figure 1a inset). This simple pattern

indicates that the surface atoms are ordered, although the arrangement between Fe and Pd is not ordered. LEIS spectra obtained after sputtering and after annealing are shown in Figure 1a. Similar to that for the polycrystalline Pd/Fe alloy, Pd segregates to the surface of Pd₃Fe(111) after annealing to 1200 K. A simple interpretation of the LEIS data with the assumption of large flat terraces leads to the conclusion that the outermost layer contains 91 % Pd and 9 % Fe. However, as we now show, STM reveals that segregation of Pd on Pd₃Fe(111) is very different from that on Pd/Ni single crystals, and an unusual segregation mechanism occurs.

STM images were obtained at room temperature after the Pd₃Fe(111) surface was sputtered and annealed to 1200 K. A small-area (8.0 nm × 8.0 nm) STM image with atomic resolution is shown in Figure 1b. Bright spot features arise from mostly monomers and dimers, with a very small amount of trimers and tetramers. The STM image was independent of the bias on the tip (−1.0 to +1.0 V). The smallest distance between adjacent single isolated bright spots is twice the nearest-neighbor spacing (0.273 nm) of Pd₃Fe(111), and the distance between two spots in a dimer is 0.273 nm. Thus, the bright spots in this STM image are single atoms, even though they appear larger than an atomic diameter. Short-range ordering forms small domains of (2 × 2) structures. The apparent height of the bright spots is about 1.2 Å. STM often

Received Date: June 5, 2010

Accepted Date: August 2, 2010

Published on Web Date: August 05, 2010

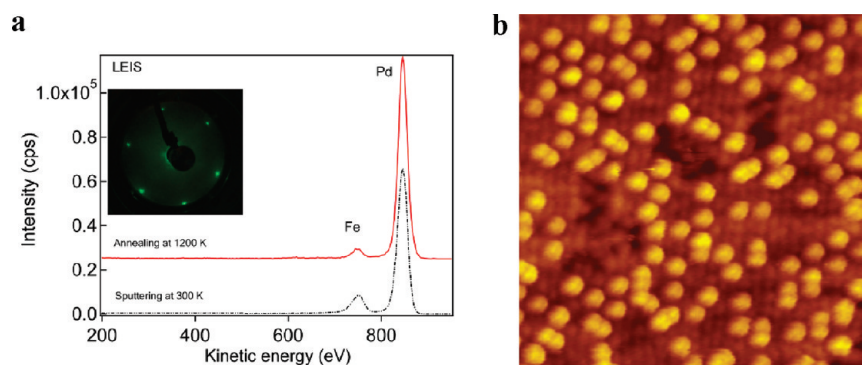


Figure 1. Pd segregation at a Pd₃Fe(111) surface. (a) LEIS of Pd₃Fe(111) before and after annealing. $E_i = 1000$ eV He⁺, 3.0 nA. Inset: LEED at $E_p = 55$ eV. (b) STM constant current topography with atomic resolution. Bright yellow spots are primarily due to segregated Pd monomers and dimers. Image size: 8.0 nm × 8.0 nm. Conditions: 1.03 mV, 2.04 nA, 0.50 Mohm.

shows very strong chemical contrast on alloy surfaces, such as in the study of Pt₂₅Ni₇₅(111).¹¹ This is attributed to an adsorbate on the STM tip, which interacts strongly with one of the components in the alloy. However, the large apparent height of the bright spots on the Pd₃Fe(111) surface is not only from the chemical contrast but mainly due to a topographic effect indicative of adatoms (and in this case, Pd adatoms, as discussed below). We observed single Pd adatoms moving across the surface, jumping from one adsorption site to the next, as they followed the trajectory of the tip (in a “pulling mode”).¹² This is shown by atoms labeled with an arrow in Supporting Information Figure 1. Examination of these atomic resolution STM images shows that the bright spots are located at positions different from lattice registries of the first layer, which eliminates the possibility that these bright spots are embedded within the first layer. Therefore, STM provides solid evidence that the bright spots are due to single atoms, dimers, trimers, and tetramers present in an adlayer. Statistical analysis of STM images (Supporting Information Figure 2) reveals that the bright spot coverage is 17%, which excludes the possibility that these bright spots are Fe adatoms since the Fe concentration is only 9% on the surface as determined by LEIS. The coverage of 0.91 ML (monolayer) Pd determined by LEIS is due to the total number of Pd atoms in the topmost (first) alloy layer and the coverage of 0.17 ML Pd present as adatoms. Atoms within the first alloy layer can be seen by LEIS because of the open structure of the adlayer. The assignment of these adatoms as Pd is consistent with the lower surface energy of Pd compared to that of Fe, which is because of the lower number of unpaired d electrons in Pd. Thus, the clean annealed Pd₃Fe(111) alloy crystal terminates in an unusual surface structure comprised of 0.17 ML Pd adatoms segregated on the outermost layer of a Pd-enriched alloy surface.

The formation of Pd adatoms at the Pd₃Fe(111) surface is surprising. The mobility of metal adatoms is expected to be high at the high temperatures used for annealing, and therefore, the adatoms might be expected to diffuse easily on terraces and accumulate at step edges because of the higher number of nearest neighbors and to cause step-flow growth. This does occur extensively on the Pd₃Fe(111) surface since high-temperature annealing removes much of the roughness induced by ion sputtering, smoothes the surface, and forms the large flat terraces imaged by STM. In order to understand

the experimental findings regarding the segregation and distribution of Pd atoms, we performed DFT calculations and directly investigated the energetics of several possible segregation pathways and diffusion barriers for Pd adatoms moving from atop sites to step edges at room temperature. At temperature T and pressure P , the stability of an ensemble is determined by its Gibbs free energy, $G(T,P)$, which is defined as¹³

$$G(T,P) = \Delta E + F_{\text{vib}} - TS_{\text{conf}} + PV \quad (1)$$

where ΔE is the total energy difference that can be conveniently obtained from DFT calculations, F_{vib} is the vibrational free energy that includes vibrational energy and vibrational entropy, S_{conf} is the configurational entropy, and V is the volume. The vibrational free energy at temperature T for a phonon with vibrational frequency ω is determined by the following equation¹³

$$F_{\text{vib}}(T, \omega) = \frac{1}{2} \hbar \omega + k_B T \ln(1 - e^{-\hbar \omega / k_B T}) \quad (2)$$

where \hbar and k_B are the Planck and Boltzmann constants, respectively. The configurational entropy for n defects on a surface with N sites is expressed as $S_{\text{conf}} = k_B \ln[N!/(n!(N-n)!)]$. Since the experiments were conducted under ultrahigh vacuum, the contribution of the last term in eq 1 is negligible. We considered four possible processes for Pd segregation, as shown in Figure 2a. In process I, a Pd atom segregates from the subsurface layer to the surface layer by exchanging its position with a surface Fe atom. This leads to Pd enrichment in the surface layer as observed in our experiment. Processes II, III, and IV are designed to understand the formation of ensembles of Pd adatoms on the terraces by taking Pd atoms from the bulk, surface, and step edge, respectively.

First, we found that the change of total energy per Pd atom through process I is $\Delta E_1 = -0.23$ eV, which indicates an exothermic process. This is because the surface energy of Fe is much higher than that of Pd,¹⁴ and segregation of Pd to the surface layer reduces the surface energy of the system. By minimizing $G(T,P)$ in eq 1, we obtained the temperature dependence of the Fe concentration (θ_{Fe}) in the surface layer (without Pd adatoms) as $\theta_{\text{Fe}} = [\exp(\Delta E_A + F_{\text{vib}})/k_B T + 1]^{-1}$,

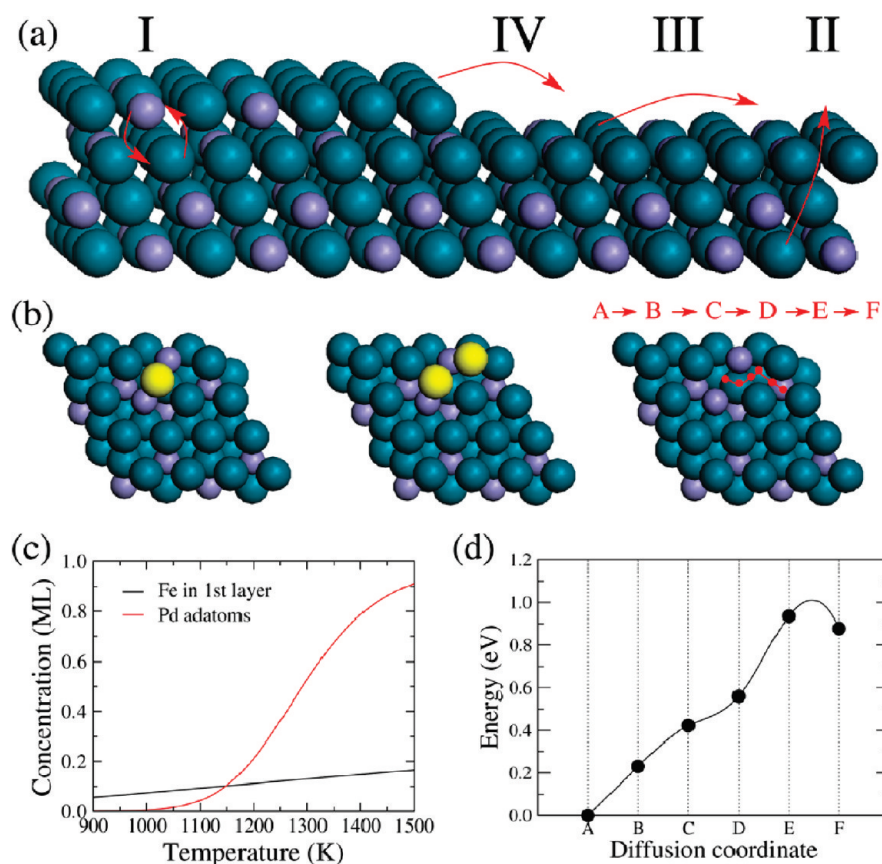


Figure 2. DFT modeling of the origin and surface structure of Pd adatoms. (a) Schematic of the segregation processes considered here. Dark cyan and medium purple balls correspond to Pd and Fe atoms, respectively. (b) Adsorption configurations of Pd adatoms as a monomer (left) and dimer (middle). The right schematic shows the diffusion path of the Pd monomer moving from site A to site F. The red dots from left to right correspond to sites A, B, C, D, E, and F in sequence. Yellow balls correspond to Pd adatoms. (c) Optimal concentration of Fe in the surface layer and Pd adatoms on the surface as a function of temperature. (d) Total energy changes when a Pd monomer adatom diffuses along the path shown in (b). Dark filled circles show the calculated energies, and the line is the fitted curve by using cubic spline interpolation.

which is plotted as the black line in Figure 2c. In the temperature range of 900–1500 K, we see that θ_{Fe} increases almost linearly from 5 to 14%. At 1200 K, the calculated value of θ_{Fe} is about 0.11 ML, which is in the range of that observed in the experimental measurements. When Pd adatoms are present, the interaction between Pd and Fe decreases the surface energy of Fe, and this would cause the calculated value of θ_{Fe} to increase.

In order to address the energetics of processes II, III, and IV, we first investigated the stability of a Pd monomer and dimer on the Pd₃Fe(111) surface, considering cases with 0–2 Fe atom(s) under the Pd adatom(s). The configuration with three Fe atoms under the Pd adatom was not considered here as it causes very high Fe concentration on the first layer, which is against the LEIS results. We found that a Pd monomer prefers a bridge site between two neighboring surface Fe atoms, as shown in Figure 2b. For this case, we found that formation of a Pd monomer through all three processes is endothermic. Particularly, the energy costs for processes II and III are as high as $\Delta E_{\text{II}} = 2.0$ eV and $\Delta E_{\text{III}} = 1.57$ eV, respectively. Therefore, these processes should hardly occur even at high temperature. In contrast, the energy cost for an

edge Pd atom to become an adatom through process IV is $\Delta E_{\text{IV}} = 0.75$ eV, and the probability for an edge Pd atom to dissociate is already reasonably high at 1200 K. This energy is further reduced by about 0.04 eV/atom when two Pd monomers bind together to form a dimer (see Figure 2b). Therefore, we believe that Pd adatom ensembles observed in our STM images are formed mainly through process IV, as depicted in Figure 2a. Using the calculated total energies for a Pd monomer and dimer with configurations shown in Figure 2b, we estimate from eq 1 that the equilibrium concentration of Pd adatoms on Pd₃Fe(111), including Pd monomers and dimers, is about 0.21 ML at 1200 K. This is slightly larger than the experimental measurement of 0.17 ML of Pd, as might be expected because some Pd adatoms may aggregate to the step edge again during cooling. In Figure 2c, one can see that the population of Pd adatoms is a steep function of temperature at around 1200 K, mainly due to the enhanced contributions of vibrational free energy and configurational entropy at high temperature.

It is known that metal atoms are mobile on close-packed metal surfaces at elevated temperatures. Hence, the stability of Pd adatoms on Pd₃Fe(111) during cooling to room

temperature is another important experimental observation to understand by using DFT calculations. Since the diffusion energy barrier of Pd adatoms on Pd(111) is just 0.35 eV,¹⁵ the stability of Pd adatoms on Pd₃Fe(111) at room temperature is mainly governed by the diffusion of Pd adatoms out of the vicinity of surface Fe. This process can be represented by the diffusion from the ground-state site (A) to a hollow site over three surface Pd atoms (F), as shown in Figure 2b. Interestingly, the energy barrier for this diffusion is about 1.0 eV, which means that diffusion of the Pd monomer is “blocked” at room temperature. In addition, diffusion of a Pd dimer is more difficult than that of a Pd monomer; therefore, Pd dimers are even more stable during the cooling process. This high stability of Pd adatoms on the Pd₃Fe(111) surface hinders the back diffusion of Pd toward step edges, as occurs on other surfaces. The origin of this blocking effect should be assigned to the large difference between Pd–Pd and Pd–Fe interactions.

Nearly quantitative agreement between theory and experiment validates our models. One can see that the exact structure and composition of a bimetallic surface, such as for Pd₃Fe(111) here, might be governed by small energy differences, for example, ~0.23 eV/atom. Synergistic exploration using experimental and theoretical approaches as described here is essential for the identification of segregation pathways and provides opportunities for the fabrication of optimized bimetallic surfaces for practical applications.

We propose a schematic model, which is shown in Figure 3b, to help visualize the surface structure of the adatoms and top alloy layer. As we have discussed, all adatoms are Pd, and therefore, 0.1 ML Fe as determined by LEIS must be within the topmost (first) alloy layer. Figure 2b shows the two most stable configurations for a Pd monomer and Pd dimer, as determined by DFT total energy calculations. In each case, there are two Fe atoms in the first layer contacting a Pd atom of the monomer or dimer; therefore, the Fe concentration in the first layer should be larger than the concentration of Pd adatoms (0.17 ML). We believe that shadowing and blocking effects by Pd adatoms might reduce the Fe signal in LEIS to indicate only 0.1 ML of Fe. The schematic model shown in Figure 3b directly corresponds to the STM image shown in Figure 3a with 32 Pd adatoms and satisfies the optimized configurations shown in Figure 2b. This model illustrates that the surface energy of Pd₃Fe(111) with Pd adatoms is lowered by heteroatomic interactions between Pd and Fe at the surface. Observations that Fe prefers to be in the second layer after annealing Fe films deposited on a pure Pd(111) crystal, as shown in Supporting Information Figures 3 and 4, provide additional support for this conclusion. Strong heteroatomic interactions are also found in other more extensively studied Pd alloy systems, for example, Pd/Ni alloys, where Pd segregation increases the amount of Pd in the first (topmost) layer on the (111) and (100) surfaces and Ni enrichment occurs in the second layer. The oscillating interlayer chemical ordering is caused by attractive Ni–Pd interactions.^{16,17} A high stability of metal adatoms caused by such heteroatomic interactions has also been reported for Ir–Rh¹⁸ and Pd–Pt systems.¹⁹

To summarize, we have discovered an unusual structure for the clean, annealed Pd₃Fe(111) surface by using a combination of LEED, LEIS, and STM. Pd atoms segregate to the

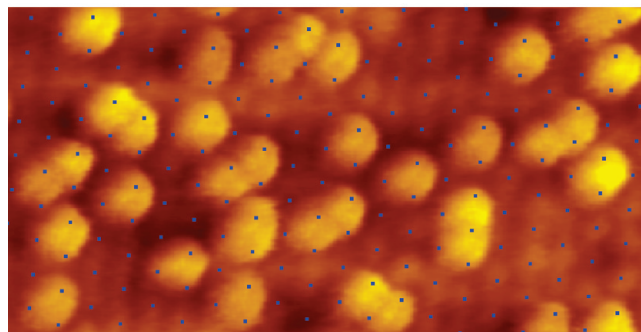
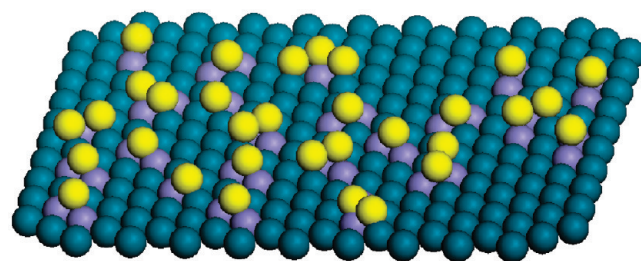
a**b**

Figure 3. STM image of 32 Pd adatoms and a corresponding schematic model including the structure of the first layer. (a) A fcc lattice is superimposed on the STM image to show the positions of first-layer atoms. (b) Schematic view of an incomplete adlayer that corresponds to the STM image, with bright yellow balls representing Pd adatoms and dark cyan and medium purple balls corresponding to first-layer Pd and Fe atoms, respectively. We are unable to determine Fe atom concentration and position in the first layer directly from the STM image, but the Fe positions indicated are estimated on the basis of DFT calculations to fit the Pd adatoms configurations in (a).

surface during annealing to 1200 K, and cooling to room temperature forms a surface with Pd monomers and dimers on top of the first layer. Such a Pd adatom structure is unusual but is thought to stem from the low surface free energy of Pd and an increased stability of Pd adatoms through localized heteroatomic interactions between Pd and Fe. DFT calculations are used to account for the stability and formation of Pd adatoms on this surface, identifying that the most likely sources of Pd are edge atoms of terraces. The specific chemistry and catalysis at this surface deserves more attention in order to explore the possible chemical and physical properties of these Pd monomers and dimers. Observation of this unusual surface structure should contribute to an improved understanding of heterogeneous catalysis of Pd-based alloys.

SUPPORTING INFORMATION AVAILABLE Details of the experimental procedure and theoretical calculations and supporting figures. This material is available free of charge via the Internet at <http://pubs.acs.org>.

AUTHOR INFORMATION

Corresponding Author:

*To whom correspondence should be addressed. E-mail: brk205@lehigh.edu.

ACKNOWLEDGMENT This material is based upon work supported by the National Science Foundation under Grant No. 0616644. Theoretical work was supported by the DOE under Grant No. DE-FG02-05ER46237, and the calculations were done on parallel computers of NERSC. B.E.K. gratefully acknowledges Dr. Radoslov Adzic for the loan of the Pd–Fe crystal.

REFERENCES

- (1) Bertolini, J. C.; Rousset, J. L.; Miegge, P.; Massardier, J.; Tardy, B. On the Large Pd Surface Segregation and Reactivity of Pd₁Fe₉₉ and Pd₅Fe₉₅ Dilute Alloys. *Surf. Sci.* **1993**, *287/288*, 346–349.
- (2) Bachir, R.; Marecot, P.; Didillon, B.; Barbier, J. Isoprene Hydrogenation on Supported Pd–Fe Catalysts: Influence of the Catalyst Preparation Procedure. *Appl. Catal., A* **1997**, *164*, 313–322.
- (3) Gucci, L. Structural Effect of Bimetallic Catalysts in the CO+H₂ Reaction. *Stud. Surf. Sci. Catal.* **1988**, *38*, 85–96.
- (4) Shao, M.-H.; Sasaki, K.; Adzic, R. R. Pd–Fe Nanoparticles as Electrocatalysts for Oxygen Reduction. *J. Am. Chem. Soc.* **2006**, *128*, 3526–3527.
- (5) Zhou, W.-P.; Yang, X.; Vukmirovic, M. B.; Koel, B. E.; Jiao, J.; Peng, G.; Mavrikakis, M.; Adzic, R. R. Improving Electrocatalysts for O₂ Reduction by Fine-Tuning the Pt–Support Interaction: Pt Monolayer on the Surfaces of a Pd₅Fe(111) Single-Crystal Alloy. *J. Am. Chem. Soc.* **2009**, *131*, 12755–12762.
- (6) Shao, M.; Liu, P.; Zhang, J.; Adzic, R. Origin of Enhanced Activity in Palladium Alloy Electrocatalysts for Oxygen Reduction Reaction. *J. Phys. Chem. B* **2007**, *111*, 6772.
- (7) Bertolini, J. C.; Jugnet, Y. Surface Structure and Catalytic Reactivity of Palladium Overlayers for 1,3-Butadiene Hydrogenation. In *The Chemical Physics of Solid Surfaces*; Woodruff, D. P., Ed.; Elsevier: New York, 2002; Vol. 10, Chapter 11, pp 404–437.
- (8) Rodriguez, J. A. Electronic and Chemical Properties of Palladium in Bimetallic Systems: How Much Do We Know about Heteronuclear Metal–Metal Bonding? In *The Chemical Physics of Solid Surfaces*; Woodruff, D. P., Ed.; Elsevier: New York, 2002; Vol. 10, Chapter 12, pp 438–465.
- (9) Baddeley, C. J. Adsorbate Induced Segregation at Bimetallic Surfaces. In *The Chemical Physics of Solid Surfaces*; Woodruff, D. P., Ed.; Elsevier: New York, 2002; Vol. 10, Chapter 14, pp 495–526.
- (10) Schmid, M.; Varga, P. Segregation and Surface Chemical Ordering — An Experimental View on the Atomic Scale. In *The Chemical Physics of Solid Surfaces*; Woodruff, D. P., Ed.; Elsevier: New York, 2002; Vol. 10, Chapter 4, pp 118–151.
- (11) Schmid, M.; Stadler, H.; Varga, P. Direct Observation of Surface Chemical Order by Scanning Tunneling Microscopy. *Phys. Rev. Lett.* **1993**, *70*, 1441–1444.
- (12) Bartels, L.; Meyer, G.; Rieder, K. H. Basic Steps of Lateral Manipulation of Single Atoms and Diatomic Clusters with a Scanning Tunneling Microscope Tip. *Phys. Rev. Lett.* **1997**, *79*, 697–700.
- (13) Reuter, K.; Scheffler, M. Composition, Structure, and Stability of RuO₂(110) as a Function of Oxygen Pressure. *Phys. Rev. B* **2001**, *65*, 035406.
- (14) Ruban, A. V.; Skriver, H. L.; Nørskov, J. K. Surface Segregation Energies in Transition-Metal Alloys. *Phys. Rev. B* **1999**, *59*, 15990.
- (15) Steltenpohl, A.; Memmel, N. Self-Diffusion on Pd(111). *Surf. Sci.* **2000**, *454–456*, 558–561.
- (16) Derry, G. N.; McVey, C. B.; Rous, P. J. The Surface Structure and Segregation Profile of Ni₅₀Pd₅₀(100): A Dynamical LEED Study. *Surf. Sci.* **1995**, *326*, 59–66.
- (17) Derry, G. N.; Wan, R. Comparison of Surface Structure and Segregation in AgAu and NiPd Alloys. *Surf. Sci.* **2004**, *566–568*, 862–868.
- (18) Kellogg, G. L. Direct Observation of Substitutional-Atom Trapping on a Metal Surface. *Phys. Rev. Lett.* **1994**, *72*, 1662.
- (19) Fallis, M. C.; Wright, A. F.; Fong, C. Y.; Daw, M. S. Trapping of a Diffusing Adatom by a Substitutional Surface Defect. *Surf. Sci.* **1994**, *311*, L717–L723.